

ESDA2012-82718

CONTROL STRATEGY FOR THE OPTIMAL OPERATION OF A SOLAR COOLING INSTALLATION

Vittorio Verda

Department of Energetics
Politecnico di Torino, Italy
vittorio.verda@polito.it

Giorgia Baccino

Department of Energetics
Politecnico di Torino, Italy
giorgia.baccino@polito.it

Stefano Pizzuti

ENEA
Casaccia, Italy
stefano.pizzuti@enea.it

ABSTRACT

In this paper, a solar cooling installation is analyzed with the aim of optimizing its performances. The system consists of vacuum solar collectors, which supply hot water to a LiBr absorption chiller. A boiler can be used to supply an additional amount of hot water in the case of insufficient solar radiation. In addition, a vapor compression chiller operates as a backup system and integrates the solar driven system in the case of large cooling request. Such system gives multiple operating options, especially at partial load. A model of the system is presented and applied to the real plant. It is shown that if a multi-objective optimization is performed, considering minimum primary energy consumption from fossil fuel and maximum utilization of the absorption system, a Pareto front is obtained. This occurs because the two objective functions are competing. A control strategy based on the use of neural networks is presented. Input variables are the solar radiation, ambient temperature and the cooling request. In this work the control strategy is adjusted in order to reach the minimum fossil energy consumption, but the same approach can be applied with other objective functions.

NOMENCLATURE

A	Heat transfer area (m^2)
A_c	Collector area (m^2)
COP_{cv}	Coefficient of performance of vapor compression chiller
c_p	Specific heat ($J/kg\ K$)
I_t	Total incident radiation (W/m^2)
K	Global heat transfer coefficient (W/m^2K)
L_e	Annual electricity required by pumps and cooling tower ($kWh/year$)

m_f	Mass flow rate of the fluid flowing in the solar collectors (kg/s)
PES	Primary energy savings ($kWh/year$)
pt	Penalty factor
Q_{boil}	Heat flux supplied by the auxiliary boiler (W)
Q_{sol}	Useful heat flux from the solar collectors (W)
Q_u	Cooling power supplied to the users (W)
T_{ia}	Temperature of fluid entering the absorption chiller ($^{\circ}C$)
T_{fi}	Temperature of fluid entering the solar collectors ($^{\circ}C$)
T_{fo}	Temperature of fluid exiting the solar collectors ($^{\circ}C$)
T_{oa}	Temperature of fluid exiting the absorption chiller ($^{\circ}C$)
T_{ru}	Temperature of fluid returning from the users ($^{\circ}C$)
T_{su}	Temperature of fluid supplied to the users ($^{\circ}C$)
ΔT	Difference between collector temperature and ambient temperature ($^{\circ}C$)
η	Collector efficiency
η_e	Average efficiency of the electricity production

1. INTRODUCTION

Solar cooling is an interesting concept to supply cooling to industrial, tertiary and civil users using a renewable energy source. An advantage related to the use of solar energy for cooling purpose is that cooling demand and solar availability generally match quite well.

Solar cooling can be obtained in several different ways, as: 1) production of electricity through photovoltaic panels, which is then used in vapor compression chillers [1]; 2) production of thermal energy in solar collectors, which is then used in

absorption [2] or adsorption [3] chillers or desiccant cooling devices [4].

Research in this field has grown in the recent years. In the last 10 years, the number of papers focused on this topic has increased of about 15% per year, with an increase of more than 50% in 2011 with respect to 2010.

The operating condition of solar cooling systems varies continuously along the year and during the day. Control is crucial to achieve high efficiencies [5], but only few journal papers in the literature are focused on this topic. In [6] the optimal control of an ejector cooling system driven by solar energy is considered. In [7] several control strategies for a solar driven absorption system are compared.

In this paper, the optimal control strategy for a solar cooling system is investigated. Despite solar cooling systems typically operate in transient conditions, here a steady state model is considered in the analysis. The reason for such simplification is that the paper is focused on the identification of the optimal target of the control system depending on the cooling demand and the ambient conditions (solar radiation, ambient temperature, etc.). These effects should be considered on the basis of reasonably long time compared to the time constant of the system (one hour for instance). Appropriate reactions to changes occurring in shorter time are obtained through selection of the control scheme, e.g. PID, and its characteristics. The values of the operation parameters which maximize the system performance are obtained in various off-design conditions. A neural network is then proposed to express the selected optimal strategy.

The proposed control strategy is then compared with that currently used for the system. The comparison is performed by considering the operating condition of hour basis.

2. SYSTEM DESCRIPTION

The solar cooling system considered as the application in this paper is installed at the Enea Research Center at Casaccia (Italy). A schematic of the systems is shown in Figure 1.

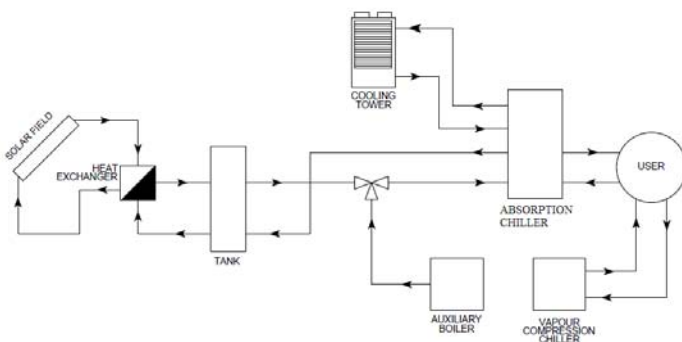


Figure 1. Schematic of solar cooling system

The system consists of a solar field, a heat exchanger, an absorption chiller, an auxiliary boiler, a hot water storage tank, two chilled water storage tanks (not shown in the Figure and

installed on the user side) and a cooling tower. The plant has been sized to provide a cooling capacity of about 60 kW. A backup vapor compression chiller is also available.

The solar field consists of 30 solar collectors (type Kloben Sky 21) with a total area of 99 m². Possible overheating due to high solar radiation and small cooling request is avoided using thermal dissipaters and, if necessary, solar screens which cover the collectors.

The thermal power produced by the collectors in reference condition is about 65 kW (solar radiation of 1000 W/m², water supply and return temperatures of 88 and 83 °C, and ambient temperature of 35 °C). A first heat exchanger is used to decouple the hydraulic circuits connecting the solar collectors and the absorption chiller.

The hot water produced on the cold side of the heat exchanger is stored in a small storage tank, which is mainly used to avoid potential quick variations in the operating conditions mainly due to possible changes in the radiation, e.g. passage of clouds. The storage tank is not considered in the following analysis, since the charge/discharge time is of the order of 10 minutes, while the control strategy is expected to be calibrated on a time period of the order of 1 hour.

Hot water should be between 75°C and 90°C to enter the absorption chiller in appropriate conditions and avoid crystallization. A heat generator allows one to increase water temperature if it is below the lower limit.

The absorption chiller is manufactured by *Yazaki*, with a nominal power of 70 kW. It uses a mixture of water and lithium bromide as the fluid process. A cooling tower is used to cool the condenser and absorber water, as well as the condenser of the backup chiller.

Table 1 shows some operating data available for the solar cooling plant. These conditions are used to calculate the unknown parameters.

Table 1 – Operating data of the solar cooling plant

Conditions	T _{fi} (°C)	T _{fo} (°C)	T _{ia} (°C)	T _{oa} (°C)	T _{su} (°C)	T _{ru} (°C)	Q _{sol} (kW)	Q _{boil} (kW)	Q _u (kW)
1	78	87	74	71.4	11.9	8.8	58.1	0.6	41
2	75.8	86.4	72	69.7	11.5	8.9	49.3	0.7	35.5
3	71	80	72	69.7	11.8	9.2	36.9	13.1	35.5
4	66	73.5	71	68.9	12.1	9.7	22.7	22.9	32.7
5	77.8	86.5	75.3	73.1	11.6	9.3	49.1	0.3	35
6	76	85	74	72	11.5	9.2	41	3.2	31.1
7	71	80	73	71.2	11.9	9.7	29.6	10.6	28.2
8	66.2	75	71	69.5	12.1	10.4	16.5	15.7	22.8
9	76	85	75.3	72.4	11.9	8.6	48.3	15.9	44.7
10	75	84.5	74	71.4	11.5	8.4	39.6	19	41
11	71	82	73	70.5	11.8	8.9	27.6	26.8	38.3
12	65	75	71	68.9	11.9	9.4	14	31.6	32.7
13	76	84.5	72	69.7	11.9	9.3	39.8	10.2	35.5
14	75	84	71.7	69.5	11.5	8.9	32.2	16.5	34.7
15	71	81.3	72	69.7	11.8	9.2	21.6	28.5	35.5
16	67	75	71	68.9	12.2	9.3	9.4	36.2	32.7

The model considered for the various components is shown in the next section.

3. SYSTEM MODEL

Solar collectors are modeled considering the energy equation

and an expression for the collector efficiency.

The heat gain of the fluid flowing in the collectors (Q_{sol}) is related to the incident solar radiation (I_T) and the gross surface area of the collectors (A_c) through the thermal efficiency (η) [8]:

$$Q_{sol} = I_T \cdot A_c \cdot \eta \quad (1)$$

The latter is dependent on the incident radiation and the difference between the average fluid temperature and the ambient temperature. A widely diffuse expression for the efficiency is:

$$\eta = \eta_0 - a_1 \frac{\Delta T}{I_T} - a_2 \frac{\Delta T^2}{I_T} \quad (2)$$

In the case of the installed collectors the manufacturer provides the following values of the parameters: $\eta_0 = 0.718$, $a_1 = 0.974$

W/m^2K , $a_2 = 0.004 W/m^2K^2$. These values are considered in this work since the expected production calculated using this model is quite close to real thermal production, as shown in Figure 2. In addition, the general approach for the implementation of a control strategy consists in a initial calibration on the theoretical performances. The strategy can be then rearranged on the basis of real performances, which may be also change because of component degradation.

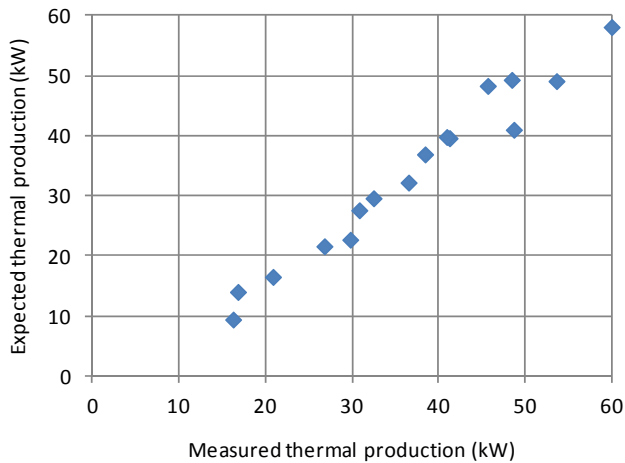


Figure 2. Calculated vs. measured thermal production of the collectors

The heat gain is used to obtain the temperature of fluid exiting the collectors (T_{fo}) to the inlet temperature (T_{fi}), the fluid mass flow rate (m_f) and the specific heat (c_p):

$$Q_{sol} = m_f \cdot c_p \cdot (T_{fo} - T_{fi}) \quad (3)$$

Heat exchanger performances have been calculated using the effectiveness – NTU approach. The heat exchanger has been modeled assuming counter flow configuration. This component divides the system in two different parts: on the hot side the solar field hydraulic circuit (water and glycol) and on the cold

side the absorption chiller supply circuit. The product of heat transfer area and global heat transfer coefficient KA is calculated in the available operating conditions (see table 1); in particular the conditions 1, 2, 5 and 6 are considered, since there is no significant heat flux supplied by the boiler. The average value of this quantity (5900 W/K) is then assumed as constant.

To model the absorption chiller, experimental curves provided by the manufacturer have been used [9]. These curves express the cooling load and the heat requirement as the function of the feeding temperature and the cooling water temperature (T_w) obtained from the cooling tower. This information can be used to obtain the coefficient of performance (COP) of the absorption chiller. This is shown in Figure 3.

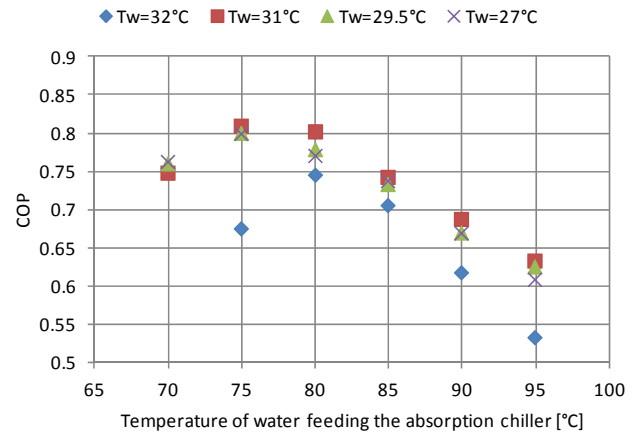


Figure 3. Chiller COP as the function of the generator inlet water temperature

The heat rejected to the cooling tower can be found by applying the energy equation to the various components.

The cooling tower is modeled using the approach available in [10], which considers ϵ -NTU equations to relate the temperature of chilled water to the inlet water temperature, its mass flow rate and the ambient conditions. In nominal conditions the air flow rate and water mass flow rate are respectively set to 3.7 m³/s and 7.6 kg/s.

The whole model has been implemented in EES [11], which allows one to easily modify the free variables and the objective function in the optimization process.

4. OPTIMAL OPERATION

Current system operation is based on constant fluid mass flow rate to the collectors and water temperature to the absorption chiller larger or equal to a minimum value. When solar radiation is small, water temperature may be lower than the minimum value. In this case the auxiliary boiler is switched on. A different control strategy is examined in this paper. System optimization is performed in order to find the best combination of the system control parameters to maximize plant performances. The operating conditions depend on solar

radiation, outdoor temperature and user requests. These input variables influence components behavior, therefore it is necessary to perform the optimization in a sufficient large set of operating conditions and determine the optimal combinations of the operating parameters in each condition.

In this work, 100 random operating conditions corresponding with different values of the input variables are considered. For these conditions, the maximum primary energy savings with respect to cooling power produced by a vapor compression chiller is considered as the objective function.

Comfort and economic aspects in system management are also considered in the analysis.

In some conditions the achievement of comfort condition leads to larger primary energy demand, due to the use of the auxiliary boiler. It is interesting to analyze the optimal conditions to allow a tradeoff between comfort that can be achieved without using the backup chillers and system efficiency.

The approach presented here is general and it is easy to replace the selected objective function with an alternative choice.

The fossil primary energy savings (PES) is calculated as the difference between the fuel consumption that would have been required by a vapor compression chiller (nominal COP of 2.8) and that required in the solar cooling system. The latter accounts for the fuel burned into the auxiliary boiler (PE_{aux}) and the primary energy associated to the electric energy required by the circulation pump and the cooling tower fans. To convert electric energy into fossil primary energy the average efficiency of the Italian thermoelectric power plants has been considered. This efficiency (η_e) is 0.46.

$$PES = \frac{\int Q_u \cdot dt}{COP_{vc} \cdot \eta_e} - PE_{aux} - \frac{L_e}{\eta_e} \quad (4)$$

The free operation variables selected in the optimization process are the solar collectors outlet temperature, the mass flow rate on the secondary circuit (i.e. the mass flow rate supplied to the absorption chiller) and the thermal power supplied by the auxiliary boiler.

Optimization has been performed using a genetic algorithm first in order to avoid local optima. The choice of a genetic algorithm has been performed despite the small number of free variables because of the quick convergence to near optimum solutions, the need to consider a large number of scenarios and the generality of the approach, which can be extended to a larger number of variables. The genetic algorithm implemented in the software EES is the Pikaia program [12]. The following parameters have been assumed in the optimization process: 64 individuals, 256 generations and mutation rate of 0.2725. The standard values of the other parameters are considered. This selection has been performed in order to explore the domain avoiding local optima. The results have been refined using the direct method of conjugate directions [13].

The multiobjective optimization has been performed by adding a penalty function to the objective function. This penalty is active if the minimum/maximum allowed value of the second

objective function is not complied (e.g. minimum cooling power supplied by the absorption chiller, Q_{targ}):

$$PES^* = PES + pt \cdot \min(Q_{abs} - Q_{targ}, 0) \cdot \Delta t \quad (5)$$

Once an optimum is obtained, the minimum/maximum allowed value is modified and a new optimum point is searched.

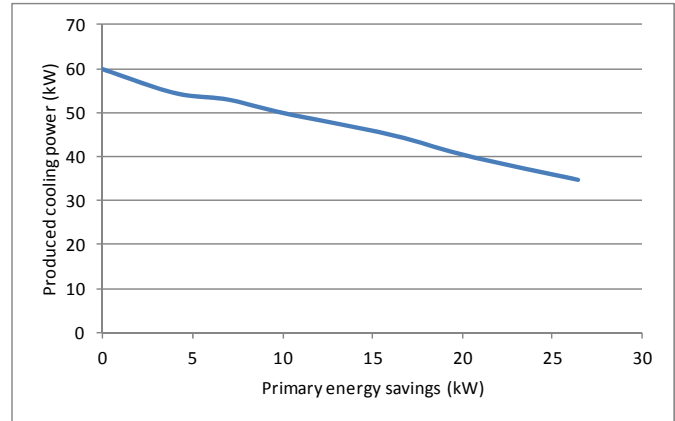


Figure 4. Cooling power product referred to primary Energy saving

The use of the auxiliary boiler increases the cooling power produced by the absorption chiller, but also the primary energy requirement of the plant.

The diagram in Figure 4 shows the results of multi-objective optimization curve corresponding to 2.8 MJ/m² incident solar radiation and to 30°C outdoor temperature. The maximum value of primary energy saving is 26.5 kW, with a cooling power product of 35 kW. In these conditions, a lower production corresponds to dissipation of solar resource. To increase the production it is necessary the use of the auxiliary boiler, so the primary energy use increases. Energy saving decreases because the marginal cooling production by the absorption chiller obtained through the use of the auxiliary boiler is less efficient than with the vapor compression chiller. The primary energy savings is positive up to an output of 60 kW. This means that, from primary energy viewpoint, the average cooling production is more convenient with the absorption chiller than with a vapor compressor unit with nominal COP of 2.8.

Diagrams in Figures 5-7 show the value of variables needed to obtain performance corresponding to points of optimum, as the function of primary energy savings.

When cooling production increases (i.e. primary energy savings decreases), the solar collector outlet temperature (plain line in Figure 5) initially decreases. This behavior depends on the decrease in the heat exchanger outlet water temperature. This results in a reduction of water temperature produced by the heat exchanger (dashed line in Figure 5). The auxiliary boiler increases the water temperature up to the value required by the absorption chiller. The average fluid temperature in the solar collectors decreases, which allows one to obtain larger heat power.

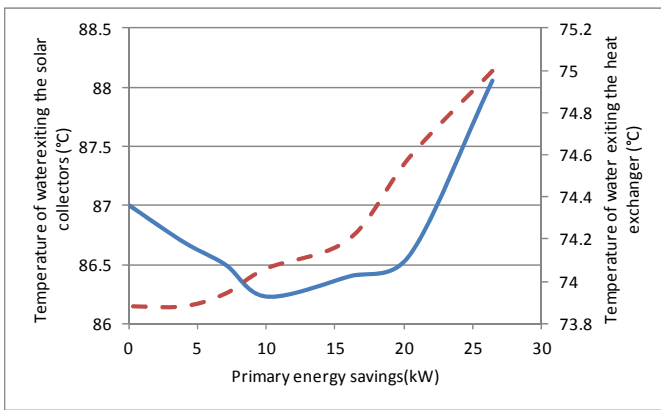


Figure 5. Solar collector outlet temperature and heat exchange outlet water temperature referred to primary energy saving.

When the cooling power increases over 50 kW, temperature of fluid exiting the solar collectors increases again.

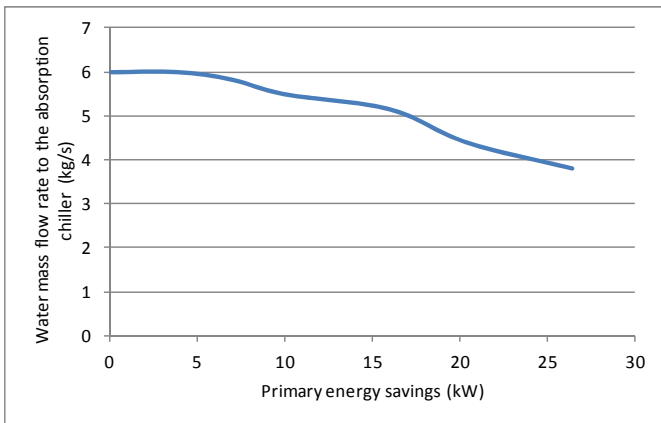


Figure 6. Water supply flow rate referred to primary energy saving.

Water mass flow rate supplied to the absorption chiller increased with increasing cooling power up to the maximum value of 6 kg/s, as shown in Figure 6.

Finally, the thermal power supplied by the auxiliary boiler increases linearly with the cooling load supplied by the absorption chiller, as shown in Figure 7.

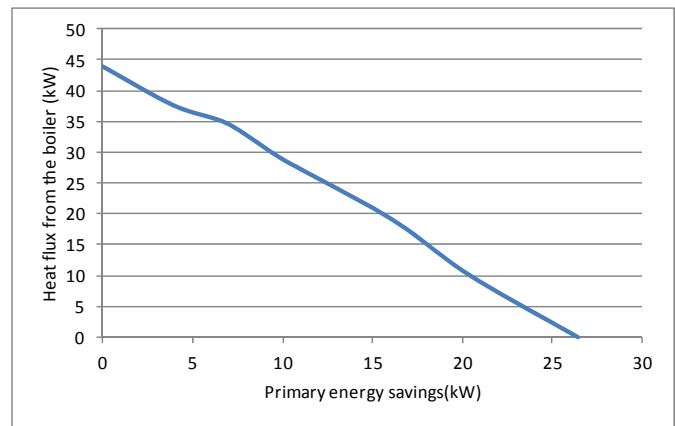


Figure 7. Thermal power of auxiliary boiler referred to primary energy saving.

5. CONTROL STRATEGY

When ambient conditions changes, the plant should be adjusted in order to guarantee acceptable performances. Here the optimization of the control strategy is investigated. The analysis is limited to the conditions corresponding to the maximum energy savings. This fact implies that absorption system generally provides only a portion of the total cooling demand. The backup vapor compressor chiller is used to cover the remaining cooling request.

The control logic currently employed is the reference for optimization. This logic is described hereafter.

The ambient temperature and solar radiation are the input for the control strategy.

The inlet water temperature of the absorption chiller is actually the first control variable. The boiler works when temperature is lower than 80°C.

The second control variable is the solar collector flow rate: the value is calculated on the basis of experimental data, shown in Figure 8. This mass flow rate is obtained starting from the available measurements of thermal power, as well as the inlet and outlet fluid temperatures. Data highlight that flow rate depends on incident solar radiation. The latter has been evaluated on the basis of the thermal power provided by solar collector and the efficiency curves.

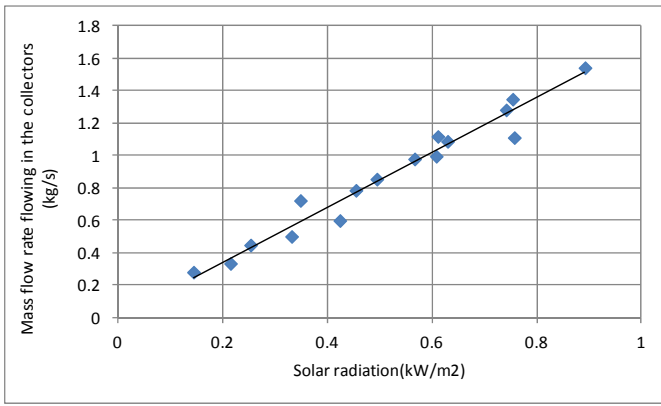


Figure 8. Solar collector flow rate referred to solar radiation.

The analysis of the optimal parameters obtained for the 100 examined scenarios shows that there is a relationship between variables too complex to implement a simple control function. Neural networks (one for each control variable) have been considered instead. The advantages of this approach are the easiness in control system implementation and the wider application possibilities. In particular, neural networks allow one to modify the objective function without modifying the control scheme but just repeating the training process. This allows one for instance to re-calibrate the control strategy on the basis of the real component performances, which may differ from the theoretical values and also change during their lifetime.

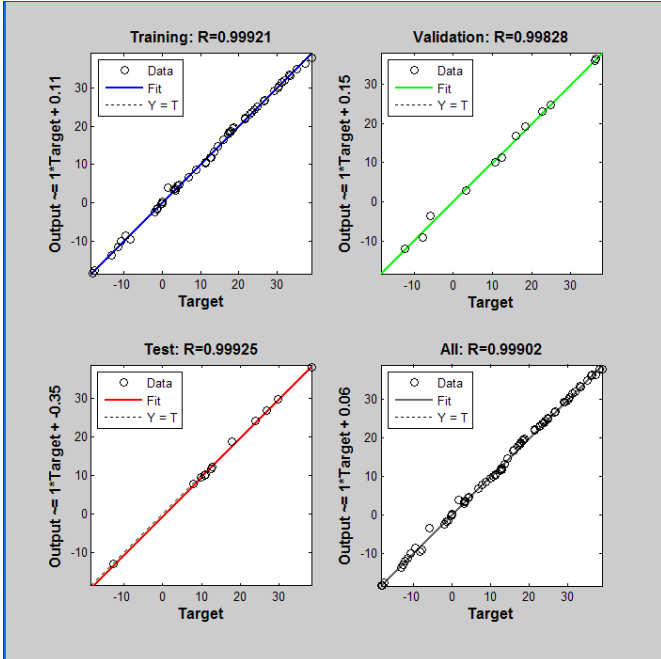


Figure 9. Comparison between exact values of the control variables and the values calculated by the neural networks

The selected scheme is a feedforward network with two layers with 7 neurons each. The first layer is constituted by neurons applying sigmoid functions, while the second layer is linear. The networks are trained with Levenberg-Marquardt algorithm [14]. The tool available in Matlab R2011 has been used.

Figure 9 shows a comparison between the real optimal values of the control variables and the values calculated through the neural network. The comparison is performed for the training ensemble (60 operating conditions), the test ensemble (20 operating conditions) and the validation ensemble (20 operating conditions). The high values of the correlation index, always over 0.99, show that the neural network constitutes an acceptable approximation of the control variables.

The comparison between the two control logics is proposed. Scenarios correspond to different solar radiations (in the range 0.1 – 1 kW/m²) and different cooling power requested by the user (in the range 25 – 50 kW). A 30°C outdoor temperature constant value has been assumed. Results are shown in Figures 10 and 11.

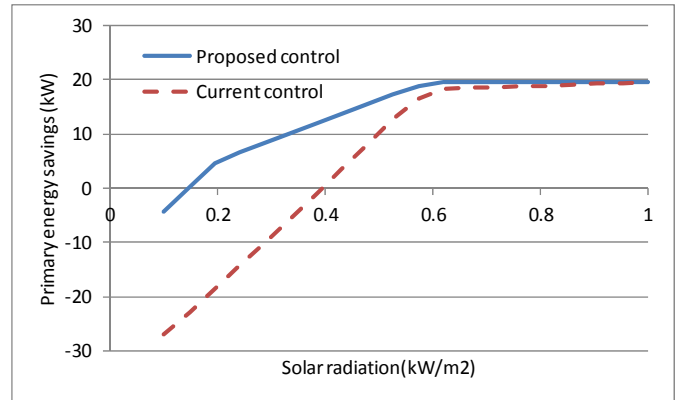


Figure 10. Primary energy saving referred to total solar radiation – power requested of 25 kW

In the case of a cooling load of 25 kW, the current control strategy (dashed line) and the proposed one (solid line) provide very similar results when the incident radiation is larger than 0.6 kW/m². In this case, the cooling power produced in the absorption chiller satisfies the request using hot water produced by the solar collectors. The auxiliary boiler does not operate.

In case of lower radiation, the proposed strategy allows one to achieve larger primary energy savings. The main reasons are:

1. In the proposed strategy, both the absorption chiller and the backup vapor compression chiller supplied cooling power to the user, while in the case of the current strategy only the absorption chiller works. As the solar radiation is not sufficient to cover the cooling request, the auxiliary boiler works.
2. There is a different use of auxiliary boiler in the two strategies: in the proposed control, the boiler is only used below a radiation of 0.2 kW/m² to keep minimum value of absorption chiller inlet water temperature.

3. There is a different set of system control parameters, which allows one to maximize the utilization of solar energy.

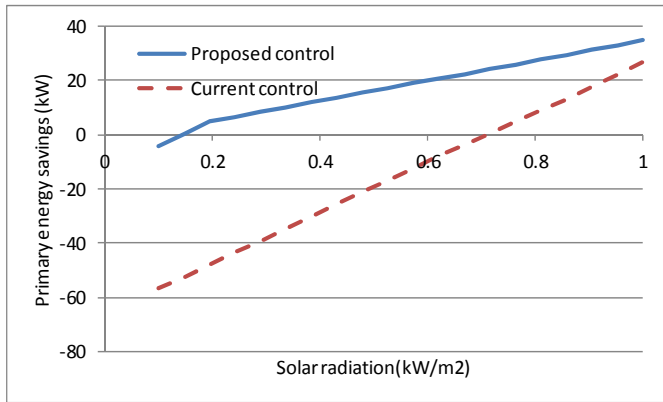


Figure 11. Primary energy saving referred to total solar radiation – power requested of 50 kW.

In the case of cooling load of 50 kW, the curve corresponding with the proposed strategy is above the curve of current strategy (see Figure 11). The current strategy (dashed line) is more convenient than the use of vapor compression chillers only in case of total radiation larger than 0.7 kW/m^2 . In the case of the proposed control strategy, the auxiliary boiler is off when the solar radiation is larger than 0.2 kW/m^2 . As in the previous case, the backup chiller is used to integrate the cooling power produced by the absorption chiller.

6. APPLICATION

In this section, the two control strategies are applied to the mathematical model of the solar cooling plant considering the cooling requests of the building F51 in the Enea research centre, near Rome. This is the building on the roof of which the solar collectors are installed, and which is connected to the cooling plant.

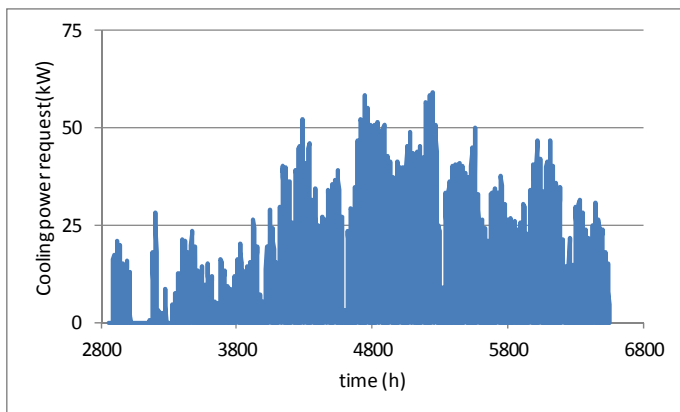


Figure 12. Cooling power demand

The cooling load of this building have been calculated using a simple model accounting for the building surface and volume,

the thermal characteristics of walls and windows, and the local climatic data. Simulations have been performed considering average hourly data.

Figure 12 shows the cooling load in the period from May to September. The maximum cooling request is 59 kW. This is registered in a day with outdoor temperature of 35°C .

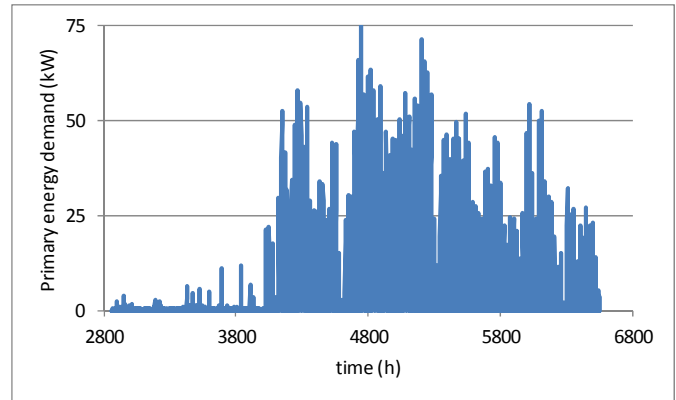


Figure 13. Primary energy demand – current regulation

Figure 13 shows the primary energy demand in the case of the current control logic. The diagram shows a peak demand of primary energy of about 75 kW.

A significant reduction in primary energy requirements occurs with proposed strategy application, as shown in Figure 14. The peak demand is reduced to about 40 kW. This is mainly achieved through larger utilization of the vapor compression chiller, but improvements are also due to the optimization of the operation of the solar collectors and the absorption chiller.

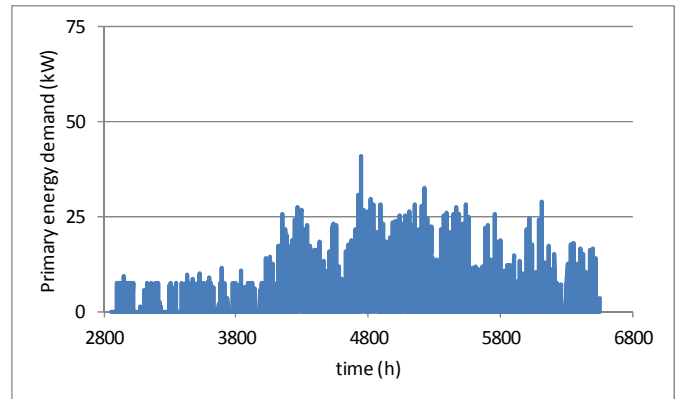


Figure 14. Primary energy demand – proposed regulation

The total annual primary energy consumption in about 17600 kWh in the case of the current control strategy and 10500 kWh in the case of the proposed control strategy. This means about 40% reduction.

7. CONCLUSIONS

In this paper, the optimal control strategy for a cooling system constituted by a solar driven absorption chiller and a backup vapor compression chiller is analyzed. This system is operating in the ENEA research center, near Rome.

The results obtained from the analysis of several scenarios allow to give a general outline in optimization for solar cooling system management. Primary energy requirements and cooling power produced by the absorption chiller have been considered in the approach as the objective functions.

The control strategy has been then developed considering the maximum energy savings as the objective function. To build the control strategy 100 scenarios corresponding to different ambient conditions and cooling request from the users. To implement the control strategy three neural networks are used to determine the values of the operation free variables as the function of the ambient conditions and request from the users.

The application to a typical cooling request from the building where the plant is installed shows that the proposed approach allows to obtain significant benefits with respect to the current strategy. This is mainly obtained thanks to a different utilization of the backup vapor compression chiller, which is used as an auxiliary system to integrate the cooling power. This is a peculiar option, that cannot be generalized to other solar cooling plants, but it shows that an appropriate design of the system is necessary. In addition, significant improvements can be obtained by optimizing the other control parameters, in particular the temperature of fluid exiting the solar collectors and the water mass flow rate directed to the absorption chiller.

8. ACKNOWLEDGEMENTS

This work has been funded within the MSE-ENEA research framework on the Electrical System, years 2008-2009, project 3.4 task C2. Authors are grateful to the ENEA personnel for their collaboration, in particular to Mauro Annunziato, Andrea Calabrese, Giuseppe Corallo and Andrea Simonetti.

9. REFERENCES

- [1] L.A. Chidambaram, A.S. Ramana, G. Kamaraj, R. Velraj (2011). Review of solar cooling methods and thermal storage options. *Renewable and Sustainable Energy Reviews* 15: 3220–3228
- [2] X.Q. Zhai, M. Qu, Y. Li, R.Z. Wang (2011). A review for research and new design options of solar absorption cooling systems. *Renewable and Sustainable Energy Reviews* 15 (2011) 4416–4423
- [3] O.StC. Headley, A.F. Kothdiwala, A. McDoom, A. (1994). Charcoal-Metanol adsorption refrigerator powered by a compound parabolic concentrating solar collector. *Solar Energy*, 53: 191-197
- [4] H-M. Henning, T. Erpenbeck, C. Hindenburg, I.S. Santamaria (2001). The potential of solar energy use in

desiccant cooling cycles. *International Journal of Refrigeration* 24: 220-229.

[5] F.G. Shinskey (1978). *Energy Conservation through control*. Academic Press. New York.

[6] B.J. Huang, C.W. Yen, J.H. Wu, J.H. Liu, H.Y. Hsu, V.O. Petrenko, J.M. Chang, C.W. Lu (2010). Optimal control and performance test of solar-assisted cooling system. *Applied Thermal Engineering* 30: 2243-2252

[7] L.A. Bujedo, J. Rodriguez, P.J. Martinez (2011). Experimental results of different control strategies in a solar air-conditioning system at part load. *Solar Energy* 85: 1302–1315

[8] J.A. Duffie, W.A. Beckman (2006). *Solar Engineering of Thermal Processes*. Wiley. New York.

[9] <http://www.yazakienergy.com/> (accessed May 2011)

[10] Liu H.H. (1999). *Analysis and Performance Optimization of Commercial Chiller/Cooling Tower Systems*. Masters Thesis, Georgia Institute of Technology

[11] <http://www.fchart.com/ees/> (accessed August 2011)

[12] <http://www.hao.ucar.edu/Public/models/pikaia/pikaia.html> (accessed August 2011)

[13] W.H. Press, S.A. Teukolsky, W.T. Vetterling, B.P. Flannery (2007). *Numerical Recipes: the Art of Scientific Computing*. Cambridge University Press.

[14] M.T. Hagan, M.B. Menhaj. Training Feed-forward Networks with the Marquardt Algorithm. (1994) *IEEE Transactions on Neural Networks*. Vol.5, NO. 6 November.